Field study of precipitation and water film dynamics on a road pavement

E. CAPORALI, F. CASTELLI & C. LORENZINI

Department of Civil Engineering, University of Florence, Italy.
e-mail: enrica@dicea.unifi.it

Abstract

The study of the very-small-scale (1-2 *m*) interaction between precipitation and impervious surfaces may be crucial for understanding the dynamics of water films and runoff during intense rainfall events. Such dynamics may be relevant in several practical problems, from road safety to urban drainage. The influence of rainfall spatial and temporal variability and surface geometry on the water depth is investigated, with reference to a road pavement, through an experimental monitoring station. This is composed by a video-camera, automatically activated during intense rainfall events through a weight switch, and a recording raingage. The monitoring station has been installed on a mountain road in the Versilia region, which is prone to very intense storms, and a first set of storm records have been collected and various post-processing algorithms tested. Preliminary analysis of such records are here presented, regarding the characteristics of both the down-slope wave propagation and the gravitational-capillary waves expansion formed by rain-drops splashes. These characteristics are indicators of the water film thickness and dynamics.

1 INTRODUCTION

The study of the dynamics of water films and runoff on road pavements during intense rainfall events may be of interest in several practical problems. The water film depth estimation is relevant in storm water management, i.e. dealing with urban drainage systems. The water depth is related to the storage dynamics on the surfaces. The distributed systems must be analysed taking into account both spatial and temporal variations (Chow *et al*, 1988). Due to the complexity of the mathematical formulation of the models, however, the urban water system is often treated as being lumped while hydrodynamic models have been often considered not suitable for practical applications (Cassar and Verworn, 1999).

Water film depth on road surfaces during intense rainstorms has been also investigated in relation to road safety problems. First investigations were related to the analysis of friction conditions met in the case of landing gear wheels (Horne and Dreher, 1963; Gray, 1963). The experiences relating to the aeronautic field have gradually begun to interest road and vehicle engineers, even though the results obtained were not directly applicable (Albert *et al*, 1966). The presence of water on road surface can have a marked effect on friction between vehicle tyres and the road. If the water level on a road surface increases beyond the point where the tyre tread and surface texture can disperse it, the amount of tyre in contact with the road is strongly reduced. In the worst case, the tyre may completely loose contact with the road, a condition known as aquaplaning (TRL, 1997). Aimed at evaluating the influence of heavy rainfalls on road safety, the European Community has funded a three years project called "VEhicle Road Tyre interaction (VERT)". Within this project, the research activity here presented has been developed.

Prediction schemes for runoff depths during rainfall should be validated by measurement. Since the water films can be of the order of the millimetre, accurate and direct measurement is not easy. Field tests on different sites are not always possible: the device should be small and it hasn't to interfere with the water film to measure (Reed *et al.*, 1985). On the other side, laboratory tests have the disadvantage of employing rainfall simulators, which introduce uncertainty in assessing the role of rainfall intensity and pattern. Among the familiar methods employed in laboratory, mention may be made of the point water level gauge: this consists of a fine needle that is lowered on the water-covered pavement. During the lowering, a high precision micrometer measure the position of the point of the needle between the moment it comes into contact with the surface of the film and the moment it touches the surface of the pavement (Laganier, 1977). More recently water film depths has been measured with twin metal wire probes connected to a wire resistance module. The voltage output increases as the electrical conductivity of the circuit containing the probe increases. Thus, as the wires of the probe become immersed in a deeper flow of water, a greater current is able to pass between the electrodes of the probe and this results in an increase in the voltage output (TRL, 1997). The point gauge has been also used within the VERT project, to measure water depths on real roads. The functioning criteria and the complex apparatus of

such a measurement system, however, prevented so far its maintaining in place for a time long enough (order of several months) to ensure the collection of data during a sufficient number of intense rainfall events. Rainfall simulators have been again used in the experiments.

In this work a procedure for evaluating water film depth in real conditions (i.e. on a real road during real rainfall events) is presented, as the measuring apparatus is not intrusive, its functioning is automatically activated by rainfall itself and no attendance is required during the recordings. The main drawback of the approach is that the measurement criteria are indirect, as it is based on the digital analysis of recorded movie clips. An estimate of water film properties is provided through the space-time analysis of the visible irregularities on the water film surface. These irregularities are mainly due to the presence of roll waves that are prevalent in terms of visible effects on the road surface during the periods of intense rainfall. A simple mathematical model is also proposed to evaluate water depth and specific discharge starting from wave velocity estimates. The surface morphology is recognised to be a fundamental factor in the evaluation of the water films kinematics, and it is analysed with a high-resolution digital elevation model.

The presentation of the measurement set-up and procedures is accompanied by the discussion of the results from recently recorded events, that allows us to first comment on the potentiality of the system and the needed refinements.

2 EXPERIMENTAL MONITORING SETUP

The monitoring station has been installed in the Versilia region (north of Tuscany) at approximately 210 *m* a.s.l. on the Province Road n.10 (Fig.1).

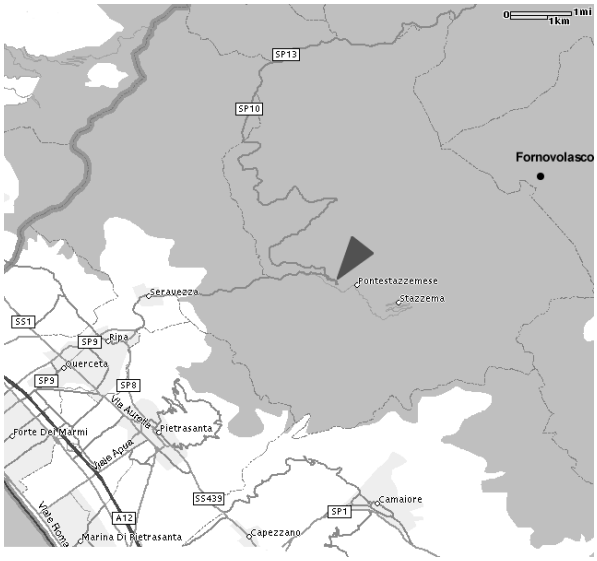

Figure 1 - Road map to the monitoring station.

The station consists of a road portion and an experimental monitoring system that is on the top of a 5 *m* pole on the edge of the road, at a distance of approximately 7 *m* from the centre of the target area (Fig. 2).

The monitoring system is composed of:

– 8-mm video camera PAL system (576 lines resolution, 25 *frames/s*).

– Tipping-bucket rain gauge with 0.2 *mm* resolution, recording on EEPROM.

– Rainfall-activated switch (experimental rainfall-weighting scale system)

The video camera is activated through the switch when rainfall intensity exceeds approximately 20 *mm/hour* (± 10 *mm/hour*). The camera viewing cone is pointed on a 1×1 *m* square painted on the ground, which is used for geometrical referencing of video clips, and it covers a total target area of about 4 m^2. Video clips are recorded on a standard 8-mm cassette, which is replaced during monthly maintenance operations. The cassette content is transformed from analogue to digital signal with a video-capturing card on a PC, allowing a nominal data-flow rate, in the current set-up, of about 2 *Mbytes/sec* (corresponding to a compression factor of about 6:1 at full 768×576 resolution and 25 *frames/sec*).

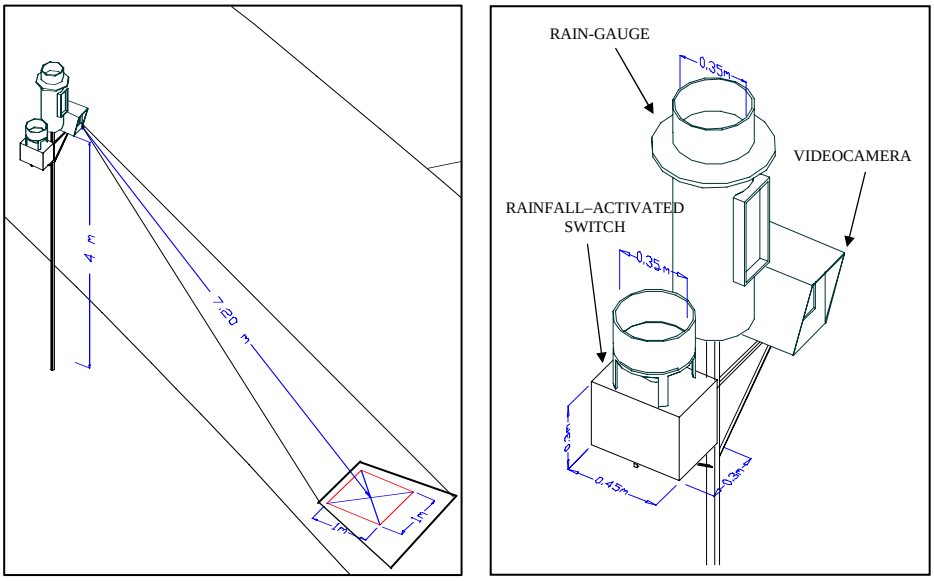

Figure 2 - Experimental monitoring station.

2.1 Road surface morphology

A description of the road surface morphology has been obtained through the construction and the coupling of two different Digital Terrain Models: a fine one, with 5×5 *cm* square cells covering a region of about 12 m^2 around the target area; a coarse one, with 50×50 *cm* square cells covering a 30 *m* long road reach to include the whole watershed for the target area. The fine DTM has been obtained from a stereo-photogrammetric survey, while a traditional topographic point-survey was used for the coarse one.

By means of standard DTM analysis, the target area has been mapped in terms of slope direction and intensity, as shown in Figure 3. Total contributing areas have been also computed for each DTM pixel with a hydrologic-type of watershed definition.

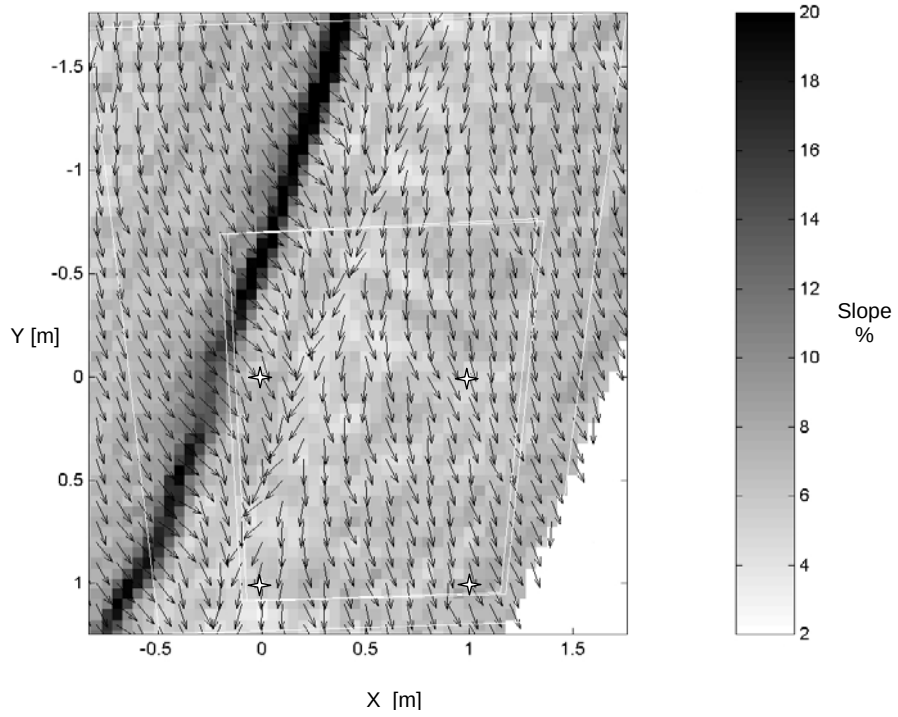

Figure 3 – Slope intensity and directions on a 5×5 *cm* grid. White frames bound the ground view of movie clips taken during different rain events.

Sensible deformations of the road pavement due to car passages (rut) can be clearly recognised inside the target area. These deformations lead to a surface geometry that is far more complex, besides the pavement roughness, than a sloped plane or a moderately curved surface. Such geometry may pose some problems in applying mono-dimensional hydrodynamic schemes such as the one described in the Appendix. Trying to overcome such difficulties, a first tentative approach has been here used in order to test the applicability of a simple mono-dimensional scheme for the roll-wave dynamics. Such approach is based on the identification of a small number of "homogeneous" regions, to be treated as distinct planar elements, each of them characterised in terms of prevalent slope (intensity and direction) and contributing area (Tab. 1). Such regions have been identified by first classifying the slope directions in 5 classes (<-01, -0.1÷0.1, 0.1÷0.3, 0.3÷0.5, >0.5 radians), then selecting clusters of contiguous pixels which, after a 5×5 median filter, belong to the same direction-class. Elongated regions are finally further subdivided for better spatial interpretation of the movie clips analysis (Fig. 4).

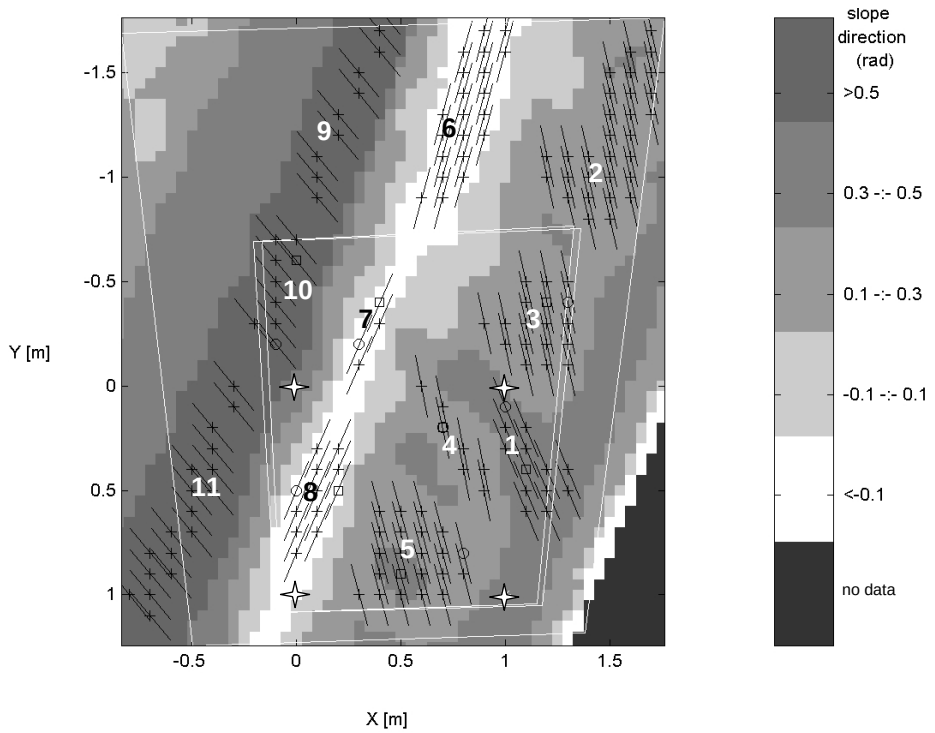

Figure 4 – Slope direction classification (5×5 median filters) and identification of 11 regions (regions 6 to 8 define the rut, regions 9 to 11 fully contribute to the water flow in the rut). Black segments define the space-time "cuts" used in the image processing procedure described in section 3.

Table 1 – Characteristic parameters of the regions.

		1	2	3	4	5	6	7	8	9	10	11
Contributing area (m^2)		0,313	0,690	0,385	0,185	0,465	0,343	0,105	0,190	0,403	0,270	0,558
Slope (%)	Mean	0,064	0,066	0,066	0,060	0,063	0,054	0,047	0,053	0,125	0,109	0,106
	St. dev.	0,009	0,008	0,008	0,010	0,008	0,009	0,005	0,007	0,059	0,045	0,035
Slope direction (rad)	Mean	0,398	0,219	0,212	0,196	0,260	-0,263	-0,406	-0,403	0,692	0,679	0,687
	St. dev.	0,097	0,122	0,113	0,102	0,119	0,188	0,218	0,295	0,259	0,194	0,153
Ln(W) (m^2/m) W = specific contributing area	Mean	-0,397	0,153	1,204	-1,148	-0,687	1,378	1,839	2,979	0,060	1,312	0,323
	St. dev.	1,638	1,666	1,491	0,833	1,131	1,510	1,539	1,393	1,294	1,312	1,285

The above identification procedures still maintain a moderate degree of subjectivity. Improvements could be obtained through the application of cluster analysis on both slope direction and intensity at different levels of filtering.

3 IMAGE PROCESSING OF VIDEO RECORDS AND WATER FILM ESTIMATION PROCEDURE

The main characteristics (average, minimum and maximum depth, discharge per unit width) of the water films, which form during intense rainfall events on the target road surface, are estimated by analysing the dynamics of laminar roll-waves. Such waves have been always observed on a large portion of the target surface when precipitation intensity exceeds values of the order of 20 *mm/hour* (average over 30 *seconds*). The estimation procedure is composed of a sequence of image processing steps and interpretation of the obtained results in terms of wave propagation velocity. A simple one-dimensional mathematical model of laminar roll-waves, described in the Appendix, is here proposed and tested to infer water film depths from measured wave velocities.

In this first phase, the procedure has been tested on data relative to four events with different characteristics in terms of duration, maximum rainfall intensity and no-rainfall frequency, recorded between July and November 1999 (Tab. 2). We here refer to the 06/11/99 event, which gave the most significant results.

The first step of the procedure is the acquisition in digital form (270×360 *pixels*, 25 *frames/sec*) of 5-*seconds* continuous samples every minute of recording. The digitalisation of the images co-ordinates of the four vertex of the 1 *m* square painted on the target road surface allows the calculation of the parameters used for the reference change from image to terrain co-ordinates system and viceversa.

Table 2 - Video-recorded events (suitable for image-processing devoted to water film depth estimation from roll-waves analysis).

Date	Time start	Duration	Mean rainfall intensity over record duration [mm/hour]	Max rainfall Intensity over a 30” interval [mm/hour]	No-rainfall Frequency over 30" intervals	Total daily rainfall [mm]
16/07/99	12:54:30	12’ 05”	55	168	0.35	22.8
27/08/99	06:04:00	12’ 00”	54	144	0.32	62.2
20/09/99	14:35:15	25’ 45”	96	192	0.12	176.2
06/11/99	13:40:45	85’ 00”	20.4	144	0.53	62.4

The image processing is based on the observation of fixed subsets of pixel positioned along a convenient direction ("cut", Fig.4) during the recording time. For each 5 *seconds* clip a 125 columns space-time diagram is obtained (Fig. 5).

As the alternation crest-trough of the waves is clearly distinguishable in terms of grey tones after a correct equalisation, this diagram allows to observe the waves crests (or the waves troughs) displacement along the chosen direction (space axis) in a time interval (time axis).

A two dimensional correlation analysis on the diagram is the tool here used to identify the direction of maximum correlation (Fig. 6), whose slope in the diagram co-ordinate system gives the estimate of the "apparent" (i.e. on the image reference frame) waves mean velocity. The apparent velocities are then re-scaled and mapped on the road reference frame through the specified co-ordinate transformation.

The cuts identification is a key-step of the procedure as it fixes the direction of the waves velocity component that is investigated and then used in the mono-dimensional hydrodynamic model. The determination of such directions is here based on morphological basis assuming the prevalent slope direction of each region as the main waves propagation direction: a sets of equal-length cuts is built inside each region along the prevalent slope direction, such that the midpoints of the segments are equally spaced (Fig. 4). A population of waves velocity estimate is thus obtained for each region in each time step (1 *minute*).

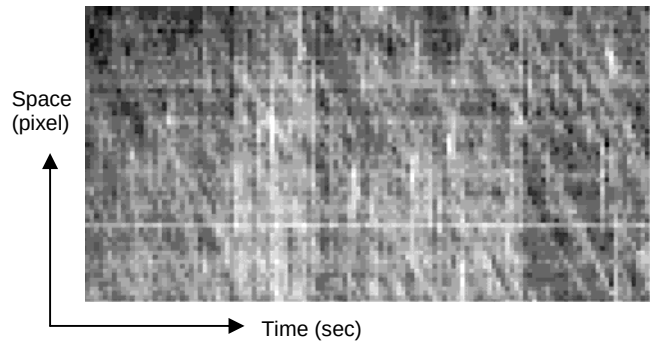

Figure 5 – Time-space diagram.

The estimated velocity are validated according to threshold criteria on correlation significance and to a minimum-maximum slope (10°÷ 85°) of the maximum correlation direction.

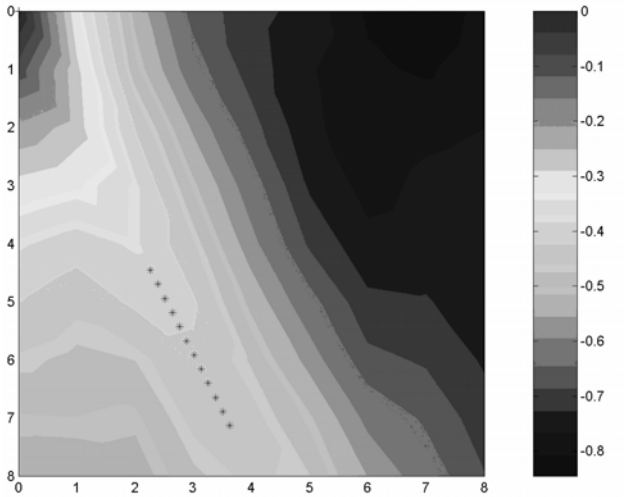

Figure 6 – Space-time correlogram.

Once the velocity estimates are obtained, the roll-wave model described in the Appendix is used to compute the values of water-depth (mean and maximum at the roll wave crest, Figures 7 and 8) and specific discharge q (discharge per unit width). Coherently with the simplified model described in the Appendix, a uniform slope is assumed inside each region, equal to the mean of the local slope intensities.

In order to perform a first consistency check of the whole procedure, we also construct a "fitted hydrologic estimate" q_h of the specific discharge series using the available in situ rainfall recording p at 30" resolution. The hydrologic estimate is based on the Nash Instantaneous Unit Hydrograph (Nash, 1957):

$$q_h(t) = A_h \int_{-\infty}^{t} p(t)h(t-\tau)dt$$
$$h(t) = \frac{t^{n-1}}{(n-1)!(t_c/n)^n}\exp(-n\cdot t/t_c) \quad (1)$$

where n has been set to 3, t_c is the concentration time and A is the specific contributing area (watershed area per unit width).

For each series corresponding to each cut we find the concentration time t_c that minimise the difference between q and q_h using a null constant linear regression (the method of moments is not suitable because the set of q values is quite sparse in time in most of the recordings).

The slope parameter of the regression line gives the "hydrodynamic" value of A_h (i.e. the value of contributing area fitted to the discharge estimates coming form the roll-wave analysis). The values of A_h for each different region can be then compared with the morphological value A_m derived for the same region as described in section 2.1.

4 COMMENTS ON FIRST RESULTS

The first results presented here, regarding the event recorded on 06/11/99, allow making some considerations on the procedure and in particular to address the limitations of the present interpretation scheme.

In both Figures 7 and 8 we observe a coherent time evolution between rainfall and estimated depths during the event in all the examined regions. Intervals with moderate or no rain corresponds to no-depth estimates, as the procedure did not recognise roll-waves phenomena. Among the cuts a Most Representative (MR, star symbols in Figure 7) has been defined with a criteria of maximisation of (first) the number of validated velocity samples inside the time sequence, and (second) the correlation among the hydrodynamic and hydrologic specific-discharge estimates.

Estimated mean water film depth in MR samples range from a minimum of about 0.3 *mm* in region 10 to a maximum of about 0.8 *mm* in region 7. A larger range, from 0.4 *mm* to 1.4 *mm*, is instead estimated for the depth at the wave crest. Among the various regions, we can see that the ones in the rut (regions 7 and 8) present bigger error-bars with respect to all the others, highlighting the complex dynamics of the flow converging there from other regions, in particular from region 10 (see Fig. 4).

The check based on the comparison with the fitted hydrologic estimate (IUH) of the specific discharge shows that the model gives different consistency of the results in different regions (Fig. 9). In some of the regions (1 to 5) we observe a smaller scatter of values along a larger dynamic range. Regions 7 and 8 in the rut present again a different behaviour, with a higher scatter on a smaller dynamic range. The comparison between the contributing specific areas computed with the morphological and the hydrodynamic approach is shown in Figure 10. We observe that, for large areas, the hydrodynamic estimate is much smaller than the morphological one, while the opposite occurs for small areas.

Such a distortion is a strong indication that either one or both of the following cases holds:

- the roll-wave scheme proposed in the Appendix does not map a measured wave-velocity range in a proper specific discharge range, i.e. it overestimates relatively small water depths and it underestimates relatively large water depths.
- possible water over-spill from one region to another has a strong influence on the water flow dynamics, so that the calculation of contributing areas on the basis of the sole surface morphology gives distorted estimates.

Discussion

The first results obtained from the experimental apparatus here described suggest that the indirect, image processing based approach is potentially suitable for obtaining detailed information on the water film dynamics on a road surface during intense rainfall events. Moreover, this information appears to contain a detailed description at short scales both in time and in space.

Another important advantage of the approach is the possibility of "capturing" a minimal set of different intense events on a single seasonal time-span. This aspect was crucial to efficiently refine the various technical aspects, not discussed here, of the experimental apparatus. These aspects ranged from reliability of unattended functioning to optimal movie shooting and sampling.

The system, however, requires the adoption of a reference hydrodynamic scheme for the transformation of the rich image information content into estimation of water film kinematic properties. The scheme adopted in the first experiments was based of a number of simplifying hypotheses, which seem to severely affect the consistency of the quantitative results. A refinement or even a substantial modification of the scheme appears then to be the next crucial step. This process will necessarily require specific laboratory experiments on the dynamics of laminar roll waves, to enrich the limited knowledge currently available on the problem.

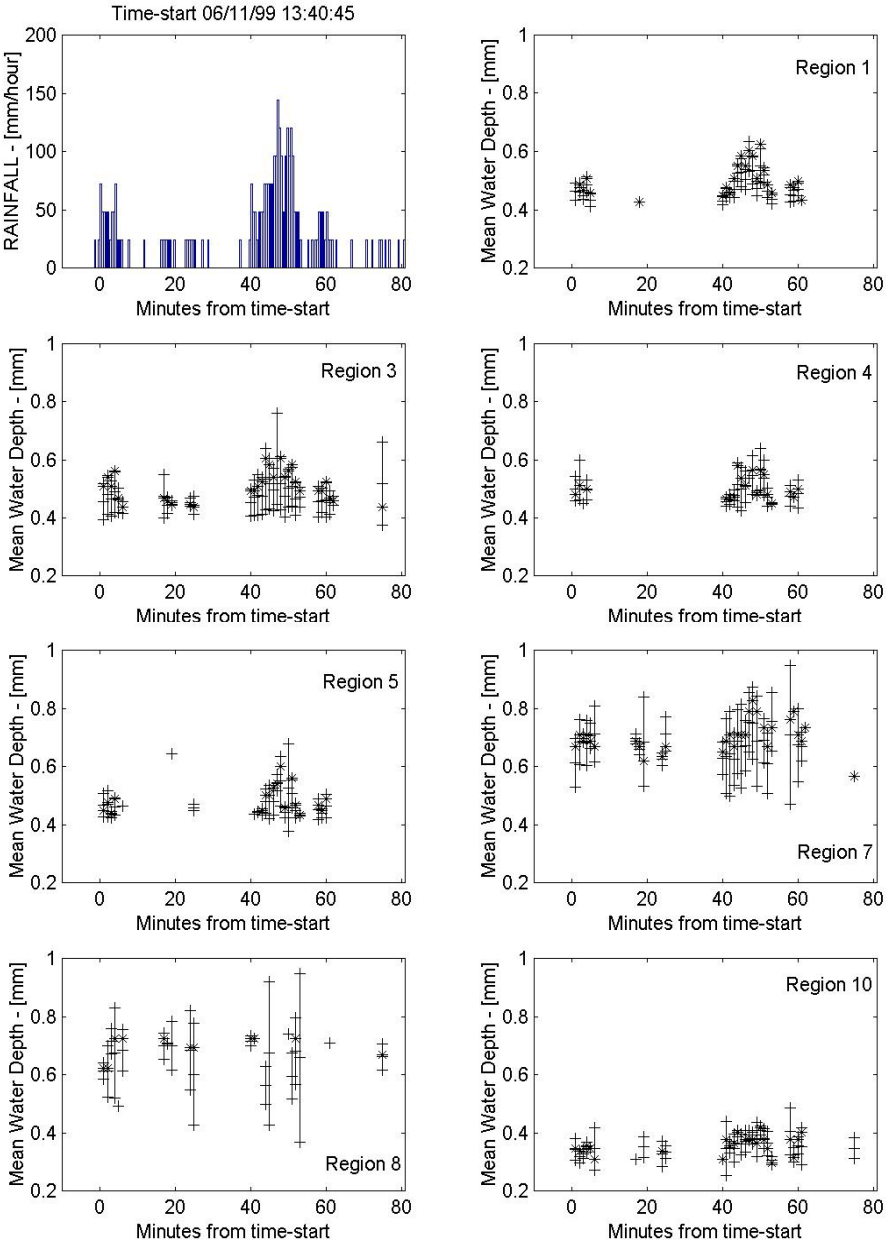

Figure 7 - Mean water depth estimations for the 06/11/99 rainfall event (upper-left panel) in the various regions of the target area. The error-bars are computed assuming a lognormal distribution for the synchronous samples inside each region. Star symbols indicate the MR samples defined in section 4.

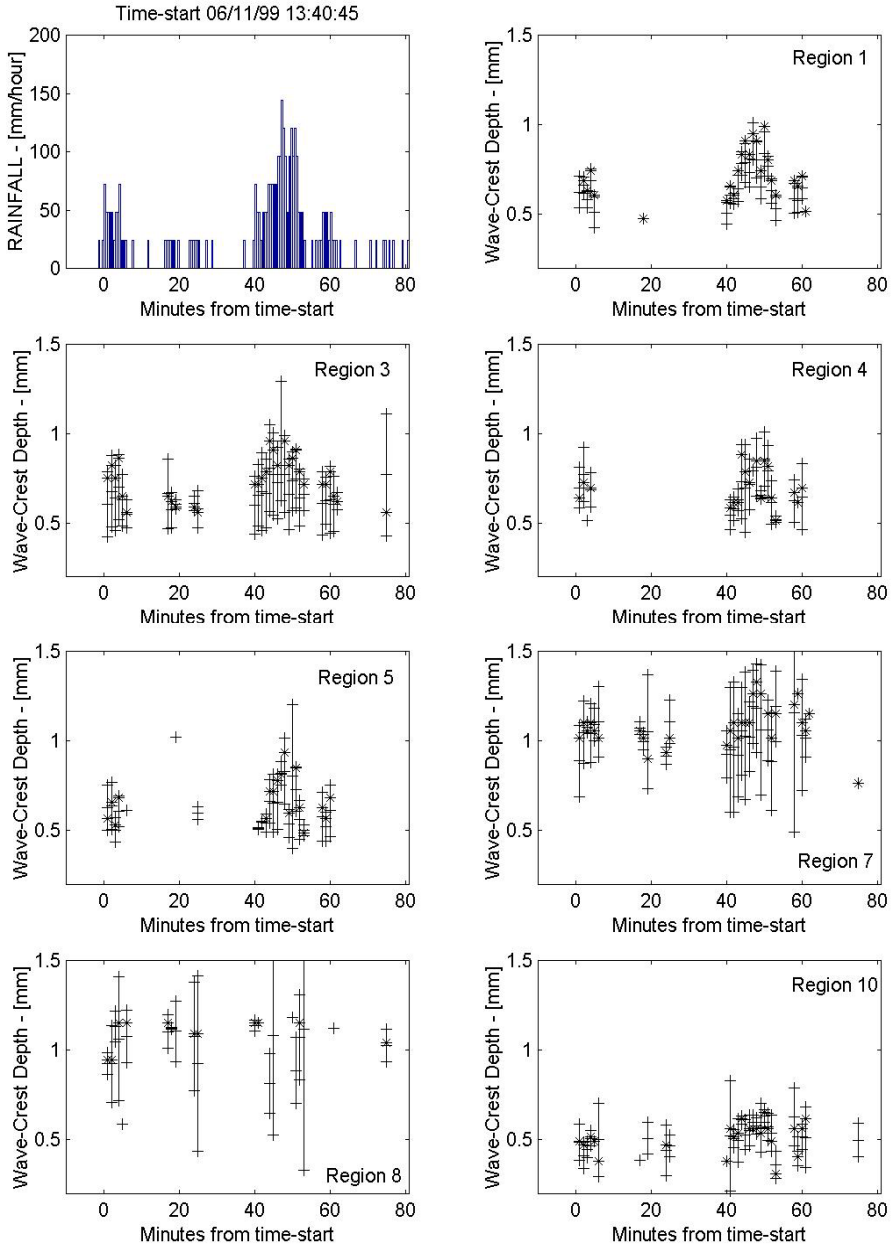

Figure 8 - As in Figure 7 but for maximum water depth (depth at the roll-wave crest).

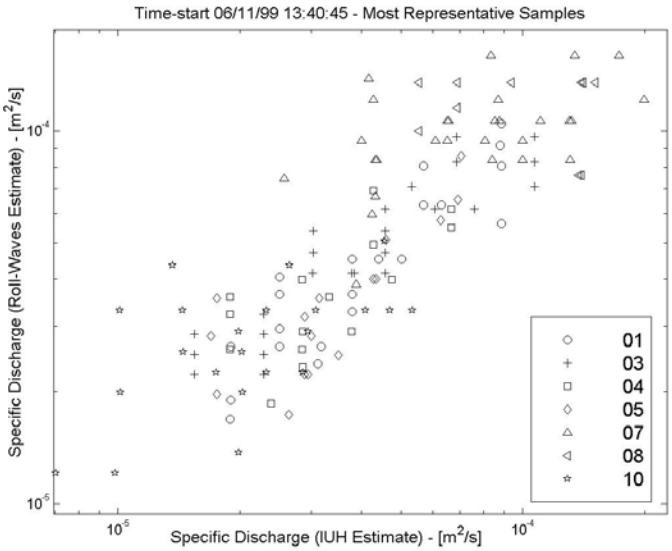

Figure 9 - Specific discharge computed with the roll-wave model vs. the specific discharge obtained with the Nash Instantaneous Unit Hydrograph during the 06/11/99 rainfall event.

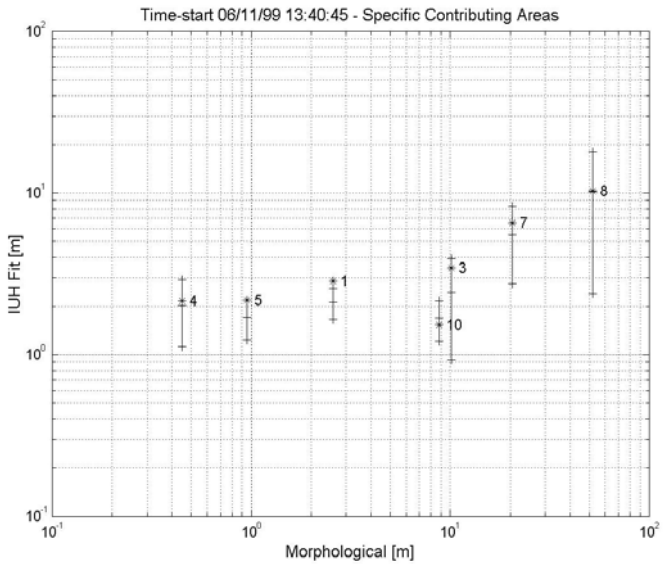

Figure 10 - The "hydrodynamic" contributing specific areas vs. the "morphological" areas in the different regions during the 06/11/99 rainfall event.

APPENDIX - Mathematical model of laminar roll-waves

Observations show that, in many cases, the fluid flow down inclined planes or channels consists of a series of steep waves at fairly long (compared to flow and wave heights) and regular intervals, named “roll waves” (Cornish, 1934; Rouse, 1938). A common feature observed in all kinds of such waves is that their propagation velocity is much higher than the one of the fluid in any region of the flow. Also, the waves velocity tends to achieve a constant value, provided that the bottom geometry and the discharge remain constant while proceeding down the slope. Early intuition by Rouse, confirmed by experimental results from Thomas (1937) and theoretical investigations by Dressler (1949), suggest that roll waves are formed in the presence of a dynamical balance between friction and gravity while, on the other hand, they can be prevented by increasing the bottom roughness.

The dynamic of roll waves has been extensively studied, both experimentally and mathematically, in the framework of fully turbulent flows. Scarcer is the knowledge of the dynamics of water roll waves in the laminar regime, i.e. in thin sheet flows (few millimetres) over moderately inclined surfaces (a few percent in slope). We start here from a mathematical model recently proposed by Kenyon (1998), whose closure was restricted to waves of infinitesimal amplitude, and we extend it to the more general and applicable case of laminar roll-waves of finite amplitude. Such a scheme will serve as the basis for the estimation of flow depth starting from wave velocity measurements.

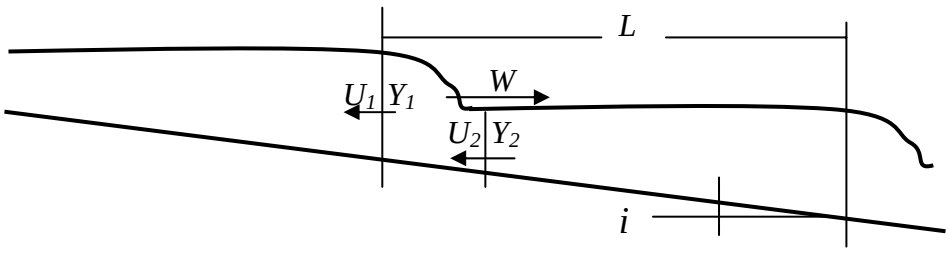

Figure A.1: Laminar roll-waves scheme.

Let us consider an inclined plane with slope i and assume that all quantities remain constant in the horizontal direction perpendicular to the slope. With reference to the qualitative flow geometry depicted in Figure A.1, we call W the wave propagation velocity, Y_1 and Y_2 the maximum (crest) and minimum (trough) flow depths and U_1 and U_2 the corresponding flow velocities relative to an observer which moves down-slope at the same wave speed W. The flow geometry remains steady in such a moving reference frame. We also assume, as always observed for such waves, that the distance between crest and trough of one roll-wave is much smaller than the distance between two subsequent crests, that is the wavelength L.

Also call g the gravity acceleration and ν the fluid kinematic viscosity. If the wavy flow is originating as an instability of an otherwise uniform laminar flow, the variations U_1 and U_2 along the vertical direction z are consistent at any depth and cannot be neglected compared to horizontal variations.

This is a main consideration that prevents us to apply the shallow water approach used in the treatment of the similar problem in turbulent flows. On the other hand, for moderate slope i, we may approximate the vertical direction as nearly orthogonal to the bottom and consider that the water profile is approximately parallel to the bottom in the crest and trough sections. This approximation allows writing, as in Kenyon (1998), a simple balance between gravity and friction in these two particular sections, with no slip condition at the bottom and no stress condition at the water surface:

$$\begin{aligned} gi &= \nu \frac{\partial^2 U}{\partial z^2} \\ U(z=0) &= C \\ \frac{\partial U}{\partial z}(z=Y) &= 0 \end{aligned} \qquad \text{(A.1)}$$

where $z=0$ defines the bottom and U is positive if directed up-slope. After defining $h=(Y_1+Y_2)/2$ as the average between the flow depths at crest and trough and $D=(Y_1-Y_2)$ the wave height, integration of the above differential problems yields:

$$\begin{aligned} U_1(z) &= W + \alpha z(z/2 - h - D/2) \\ U_2(z) &= W + \alpha z(z/2 - h + D/2) \end{aligned} \qquad \text{(A.2)}$$

where $\alpha=gi/\nu$. A first important relation may be drawn from a simple mass balance, considering constant discharge when observed in the moving reference frame:

$$\int_0^{Y_1} U_1(z)dz = \int_0^{Y_2} U_2(z)dz \qquad \text{(A.3)}$$

which yields:

$$W = \alpha h^2 \left[1 + \frac{1}{3}\left(\frac{D}{2h} \right)^2 \right] \qquad \text{(A.4)}$$

In the mentioned study of Kenyon, the problem is further addressed introducing the energy balance along the horizontal direction. This balance, however, can be made explicit in terms of the above introduced quantities only in the limit of vanishing wave height. To avoid this limitation, we consider the momentum equation in integral form in the control volume defined between the crest and trough. Given the usually observed small distance between these two sections, we may neglect the bottom friction and fluid weight, in this small reach, when compared to the pressure difference and momentum fluxes, that is:

$$\frac{g}{2}Y_1^2 + \int_0^{Y_1} U_1^2(z)dz = \frac{g}{2}Y_2^2 + \int_0^{Y_2} U_2^2(z)dz \tag{A.5}$$

Inertial terms also disappear because of the steady flow configuration in the moving reference frame where the above equation is written.

This is equivalent to the assumption, which is coherent with the first observations of Rouse, that the roll wave resemble a hydraulic jump when the wave is observed in the moving reference frame. Solving the integral, the following polynomial equation is obtained:

$$\begin{aligned} &\frac{4}{3}\alpha^2 h^4 D + \frac{2}{3}\alpha^2 h^2 D^3 + 2ghD + \frac{1}{60}\alpha^2 D^5 + \\ &+ 2W^2 D - 4W\alpha h^2 D - \frac{1}{3}W\alpha D^3 = 0 \end{aligned} \tag{A.6}$$

Coupling this equation with the previous expression of *W*, we obtain the two needed relations *W(h)* and *D(h)*:

$$\begin{aligned} D^2 &= 4\left(\frac{1}{\alpha}\sqrt{15h\left(16\alpha^2 h^3 - 3g\right)} - 15h^2\right) \\ W &= \sqrt{\frac{5}{3}h\left(16\alpha^2 h^3 - 3g\right)} - 4\alpha h^2 \end{aligned} \tag{A.7}$$

Once the wave propagation speed *W* is known together with the slope geometry, the minimum and maximum water depths can be easily computed by solving for *h* and *D* the above equations. Existence of the roll-wave configuration is however possible only if:

$$h > \left(3\frac{g}{\alpha^2}\right)^{1/3} \tag{A.8}$$

As an example, for a slope *i=5%* and usual viscosity values for water, one would obtain as a necessary condition for the formation of roll waves *h>0.5mm*. This is, however, a necessary but not sufficient condition for the formation and persistence of the roll-wave configuration. A more strict and likely sufficient one is the supercritical condition, that is a Froude number larger than one. If one approximate *h* as the actual average flow depth and consider the corresponding uniform laminar mean velocity $\alpha h^2/3$, the Froude number would be $Fr = \alpha h^{3/2}/3g^{1/2}$. The condition *Fr>1* would bring, for *i=5%*, *h>0.7mm*.

The above theoretical results may well explain why, as often observed the mean water depth of the sheet flow on a sloped road pavement does not increase much with increasing rainfall intensity. The mathematical scheme presented above may be easily used to compute the average discharge per unit width *q* (average specific discharge). Before expressing it, we need to consider that the instantaneous discharge at a fixed point in space is a quantity that varies periodically in time with period *L/W*. It will be maximum at crest passage and minimum at trough passage. To compute its mean, we only need to average the instantaneous values over a period *L/W*. This mean value can be conveniently expressed as (Dressler, 1949):

$$q = \frac{W}{L}\int_0^L Y(x)dx - \int_0^Y U(z)dz \tag{A.9}$$

The second integral on the right-hand side is, by continuity in the moving frame, independent on position. Assuming as a first approximation a linear variation of depth between trough and subsequent crest, the following result is easily obtained:

$$q = Q\left[1 + 3\left(\frac{D}{2h^2}\right)^2\right] \tag{A.10}$$

where $Q=\alpha h^3/3$ is the discharge a uniform laminar flow would attain with the same depth *h*. For fully developed roll-waves, the wave height *D* is usually observed to be of the same order of magnitude or larger than the mean depth *h*.

Then, for a given mean depth *h*, a fully developed roll-wave configuration may deliver up to four times the water of a depth-equivalent uniform laminar flow.

ACKNOWLEDGEMENTS

This research has received support from the European Community under the Brite-Euram Programme, VERT project (n° BE97-4306), contract n° BRPR-CT97-0461.

Authors would like to thank prof. Ignazio Becchi and prof. Lorenzo Domenichini for suggestions and helpful discussions. Thanks to dr. Francesca La Torre and dr. Neri Di Volo for the precious support and thanks also to Mauro Gioli, Muzio Mascherini and Daniele Ostuni for their technical contribution to the experiment.

REFERENCES

Albert B. J., Walker J.C., and Maycock G., Tyre to wet road friction, The Institution of Mechanichal Engineers, Automobile division, proceedings, 1965-1966, Vol. 180, Part 2 a, No. 4, London, 1966.

Cassar, A., Verworn, H., Modification of rainfall runoff and decision finding models for on-line simulation in real time control, Water science and technology, **39**(9), 201-216, 1999.

Cornish V., Ocean Waves and Kindred Geophysical Phenomena, Cambridge University, London, 1934.

Chow, V. T., Maidment D. R. and Mays L.W., Applied Hydrology, McGraw-Hill Book Company, 1988.

Dressler R. F., Mathematical Solution of the Problem of Roll-Waves in Inclined Open Channel, Communications on Pure and Applied Mathematics, N.Y. University, 149-194, 1949.

Gray W.E., Aquaplaning on runaways, Journal of the Royal Aeronautic Society, Vol. 67, May, 1963, London.

Horne W.B. and Dreher R.C., Phenomena of Pneumatic Tire Hydroplaning, NASA Technical Note TN D-2056, Washington, 1963.

Kenyon, K. B., Roll Wave Theory, Physics Essays **11**(4), 531-540, 1998.

Laganier, R., Skid resistance and water film thickness, from “Skidding accidents” – Ancillary Papers, Transportation Research Board, National Academy of Sciences, 1977.

Nash J.E., The form of the instantaneous unit hydrograph, IASH publication **45**(3-4), 114-121, 1957.

Reed, J.R., Kibler, D.F., Huebner R. S., Marks, G.W., Prediction of hydroplaning potential from runoff characteristics of highway pavements, The Pennsylvania Transportation Institute, Pennsylvania, 1985.

Rouse H., *Fluid Mechanics for Hydraulic Engineers*. McGraw-Hill New York, 1938.

Thomas H. A., Hydraulics of Flood Movement in Rivers, Carnegie Institute of Technology, Pittsburgh, Pa., 1937.

TRL (Transport Research Laboratory), Water depths on wide carriageways – A laboratory study, Unpublished Project Report, 1997.